November 1985 LRP 278/85

IMAGING METHODS FOR THE OBSERVATION OF PLASMA DENSITY FLUCTUATIONS

H. Weisen

Submitted for publication to Plasma Physics and Controlled Fusion

IMAGING METHODS FOR THE OBSERVATION OF PLASMA DENSITY FLUCTUATIONS

H. Weisen

Centre de Recherches en Physique des Plasmas
Association Euratom-Confédération Suisse
Ecole Polytechnique Fédérale de Lausanne
21, av. des Bains, CH-1007 Lausanne, Switzerland

Abstract

Imaging techniques offer attractive alternatives to small-angle Thomson scattering for scale lengths of density fluctuations causing diffraction in the Raman-Nath regime. This is the case for fluctuations with wavelengths above about 3 mm for tokamak sized plasmas, when a CO_2 laser probe beam is used. Four methods ("phase scintillation", phase contrast, wavefront shearing and interferometry) are compared, on the basis of their transfer properties. They offer new means of studying density fluctuations of magnitude up to the dimensions of the plasma, such as those associated with turbulence, magnetic islands, convective cells or driven waves. The long wavelength limitations are discussed in detail and are related to those encountered for far-field techniques. An experimental comparison of "phase scintillation" and phase contrast is given, and the criteria relative to the depth of field of imaging instruments in this context are considered.

1) Introduction

When the diffraction of laser light by refractive perturbations in the plasma occurs in the Raman-Nath regime (KLEIN and COOK, 1967; BORN and WOLF, 1959), the effect of the latter on the transmitted wavefront is entirely described by the usual line integrated phase shift

$$\phi(x,t) = 2\pi\lambda^{-1} \int (n_{(x,z,t)}-1)dz,$$

where $n=(1-\omega^2_p/\omega^2)^{1/2}$ is the plasma refractive index,

$\simeq 1-2.81\cdot10^{-13}\ \lambda\ n_e$ for $\omega \gg \omega_p$

$\lambda = 2\pi/k_0$ is the probe beam wavelength (cm)

$n_e = n_{e(x,z,t)}$ is the electron density (cm^{-3}).

An imaging interferometer having a wide enough access to the plasma can provide a measurement of $\phi(x,t)$ (HUGENHOLTZ and MEDDENS, 1982; YOUNG et al., 1985). As we will see however, for most of the cases of interest for the study of fluctuations, simpler near field (SHARP, 1983) or imaging methods (WEISEN, 1982, 1985) provide equivalent information.

The widely used far field (scattering) techniques on the other hand provide a measurement of the various components of $\tilde{\phi}(k,t)$, the Fourier transform of $\phi(x,t)$ (SLUSHER and SURKO, 1980; EVANS et al., 1982; TFR GROUP and TRUC, 1984; SONODA et al., 1983). Obviously the two classes of methods provide equivalent information if one is able to measure $\phi(x,t)$ at "all" positions (using a detector array), respectively $\tilde{\phi}(k,t)$ for all k. Fundamentally, the two classes and their numerous variants differ only by how and where the desired information contained in the transmitted (including diffracted) beam is extracted. However, these methods are not

necessarily equally well suited in a particular context. The most important is the choice of the probe beam parameters: width and wavelength. The total amount of information collected by the beam increases with its width. For imaging techniques an increased width reveals more of the plasma, and for scattering it results in enhanced wavenumber resolution.

Generally, for the case of scattering, one wishes to observe a homogeneous plasma sample to obtain the fluctuation's power spectrum $S_{(k,\omega)}$ and is therefore restricted to a beam width much smaller than the plasma radius. The resulting conflict with the desire for good wavenumber resolution limits the usefulness of scattering techniques at long wavelength. (The finiteness of the beam width is effectively a measurement of the position of the fluctuations observed and is therefore incompatible with a simultaneous measurement of their wavenumber.)

In well designed imaging systems this problem does not arise because no attempt to measure k is made during the recording process, and the beam width is made as large as possible. One is still free à posteriori to express the information recorded in terms of spectra. Whether this is useful or not depends on the nature of the fluctuations. It is more informative for example to view localised or complicated wave patterns directly in real space.

Thus imaging techniques appear to be preferable at long wavelength (say $\Lambda > 1$-2 cm for tokamak sized plasmas) whereas common scattering is more adequate for short wavelengths, in particular for the Bragg regime, which is not discussed here. A detailed comparison between a representative of each class ("phase scintillation" (SHARP, 1983) and far forward scattering (EVANS et al., 1982)) has recently been given by JAMES & YU (1985).

The techniques presented in the following sections will remind the reader of the Schlieren (and related) methods used on high density plasmas (JAHODA, 1971). Schlieren methods however are described by a geometrical optics treatment, the validity of which breaks down in the context of fluctuations in the low refractivity plasmas characteristic of current tokamaks, making a wave-optics treatment necessary.

2) Imaged detection of small phase shifts

Consider a plane wavefront of complex amplitude $B_{(x)}$ propagating through a thin phase object located at the plane Σ_1 (fig. 1a).

The transmitted beam $B'_{(x,t)}$ (fig. 1b) is then ($\Delta \to 0$)

$$B'(x,t) = \exp\left(i\phi_{(x,t)}\right) B_{(x)} \simeq \left(1 + i\phi_{(x,t)}\right) B_{(x)} \quad \text{for } |\phi| \ll 1. \qquad (1)$$

The intensity is not affected. However we obtain a ϕ dependent intensity $I_{(x,t)}$ if we add a reference beam $iB_{(x)}$ to an image of $B'_{(x,t)}$ (fig. 1c):

$$B''(x,t) = B'(x,t) + iB_{(x)} \quad , \text{ thus } I_{(x,t)} = 2B^2_{(x)} \left(1+\phi_{(x,t)}\right). \qquad (2)$$

This is simply the case of a homodyne interferometer tuned to fractional fringe observation, i.e. offset to the steepest point on a fringe. Other methods do not use an external reference. How is information about $\phi_{(x,t)}$ obtained in these cases ?

One answer is that by modifiying in some way the relative phasings of the large undiffracted part $B_{(x)}$ and the small diffracted part $i\phi_{(x,t)}B_{(x)}$ detectable interference of the two components can be obtained (fig. 1d). The phase contrast method (ZERNIKE, 1935; BORN and WOLF, 1959; PRESBY and FINKELSTEIN, 1967) relies on the separation of the

two components in the far field of a lens to achieve a $\pi/2$ phase shift between them and then on their recombination to form an image again. Complex amplitude and intensity are then

$$B''(x,t) = B(x)\,(1 + \phi(x,t)) \;,\; I(x,t) = B^2(x)(1 + 2\phi(x,t)). \qquad (3)$$

"Phase scintillation" (SHARP, 1983) can be considered to rely on the fact that diffracted light has a longer path to travel, from Σ_1 to the detection plane Σ_2 (fig. 1a), because it travels at a slight angle, thus building up phase differences and intensity variations that are functions of z and k.

Obviously a device without a separate reference beam cannot measure absolute phase variations like an interferometer. Therefore the phase at a given point can only be given with respect to the phase at other points in the beam, for example a weighted average over surrounding points (WEISEN, 1985). As these imaging devices are linear systems, their performances will in the following be evaluated on the basis of their transfer properties.

3) Transfer properties

The theoretical framework used to analyse imaging systems is found in basic textbooks, e.g. GASKILL (1978). The overall effect of the system on the optical wavefields is described by a linear operation $\mathcal{L}$ relating the complex amplitudes in the input (object) plane to those in the output (detection) plane.

$$\mathcal{L} : B'(x,t) \rightarrow B''(x,t) = R(x) + D(x,t) \qquad (4)$$
$$B(x) \rightarrow R(x)$$
$$i\phi(x,t)B(x) \rightarrow D(x,t)$$

It is the interference between $R_{(x)}$ and $D_{(x,t)}$ that is of interest to us because it leads to intensity variations $\Delta I_{(x,t)}$ that depend linearly on $\phi_{(x,t)}$ and can be recorded using power sensitive detectors.

$$\Delta I_{(x,t)} = R^*_{(x)} D_{(x,t)} + D^*_{(x,t)} R_{(x)}. \qquad (5)$$

The linear relation between $\Delta I_{(x,t)}$ and $\phi_{(x,t)}$ is conveniently described by introducing an instrumental impulse response $h_{i(x,y)}$ obtained by replacing $\phi_{(x,t)}$ by $\delta_{(x-y)}$ in eq. (5). The Fourier transform of $h_{i(x,y)}$ with respect to u=x-y can be interpreted as a wavenumber response (which may be position dependent). It is a transfer function, noted $H_{(k)}$, when the system is shift invariant, i.e. when $h_{i(x,y)} = h_{i(x-y)}$. Even though treating a finite system as being shift invariant is clearly an idealization, $H_{(k)}$ provides an excellent basis to compare different methods.

3.1) Phase contrast

A wave optics treatment of the phase contrast method has recently been published elsewhere (WEISEN, 1985). The above mentioned $\pi/2$ phase shift between diffracted and undiffracted light is achieved by introducing a phase plate P into the focus of lens L_1 (fig. 2). The phase plate can consist of a transparent disc having a groove of a depth such that the diffracted light falling beside it is retarded by $\lambda/4$ with respect to the undiffracted part focussed onto the groove. Lens L_2 then forms an image of the plasma at Σ', where the phase shifts produced in Σ are revealed as corresponding intensity variations. If $B_{(x)}$ is the incident beam amplitude in Σ and $C_{(x)}$ the inverse Fourier transform of the charateristic

function $\tilde{C}_{(k)}$ of the phase plates groove (fig. 3), the intensity distribution (power density) in Σ' is

$$I_{(x)} = I_{0(x)} + \Delta I_{(x)} \quad \text{(to first order in } \phi\text{)},$$

$$\Delta I_{(x)} = 2\{[B_{(x)} \otimes C_{(x)}]\, \phi_{(x)} B_{(x)} - B_{(x)}[(\phi_{(x)} B_{(x)}) \otimes C_{(x)}]\}. \qquad (6)$$

A $\otimes$ designates the convolution operation. $\Delta I_{(x)}$ is essentially proportional to the difference between $\phi_{(x)}$ and a weighted average of $\phi_{(x)}$ over neighbouring points. For fluctuation scales smaller than the scale of $C_{(x)}$ this average tends to zero and $\Delta I_{(x)}$ is directly proportional to $\phi_{(x)}$. (To simplify the notation we drop the explicit temporal dependence of $\phi_{(x,t)}$ and write the position variable $x=(x_1,x_2)$ as a scalar.)

Eq. (6) leads to an instrumental impulse response given by

$$h_{i(x,y)} = 2B_{(x)}\,[B_{(x)} \otimes C_{(x)}]\,\{\delta_{(x-y)} - \frac{B_{(y)} C_{(x-y)}}{B_{(x)} \otimes C_{(x)}}\} \qquad (7)$$

which in the shift invariant approximation (around x=0) reduces to (fig. 4.b')

$$h_{i(x-y)} = h_{i(u)} \simeq 2I_0\,\{\delta_{(u)} - \frac{B_{(-u)} C_{(u)}}{\int B_{(v)} C_{(v)} dv}\} \qquad (8)$$

where $B_{(x)}[B_{(x)} \otimes C_{(x)}] \simeq I_{0(x)}$.

The corresponding transfer function is

$$H_{(k)} = 2I_0\,\{1 - \frac{\tilde{B}_{(-k)} \otimes \tilde{C}_{(k)}}{\tilde{B}_{(-l)} \otimes \tilde{C}_{(l)}\big|_{l=0}}\}. \qquad (9)$$

The behaviour of $H_{(k)}$ is depicted in fig. 3 for the experimentally representative case where both $\tilde{B}_{(k)}$ and $\tilde{C}_{(k)}$ are even functions. For $k > k_c$, $H_{(k)}$ is essentially flat, as for an interferometer. The cutoff wavenumber k_c can be chosen sufficiently small to allow detection at wavelengths of the order of the diameter of the beam.

In the case of Raman-Nath diffraction the k-spectra are symmetrical and both halves carry the same information. It is also possible to obtain transfer properties very similar to those of phase contrast by suppressing half of the diffracted spectrum while leaving the undiffracted part unaffected and use it as a local oscillation in Σ'. Although very different in interpretation this strongly resembles the Knife Edge Schlieren method (JAHODA, 1971). As its sensitivity is reduced by $^1/_2$ compared to phase contrast, it will not be considered further here.

3.2) Phase scintillation

We now give a brief treatment of the case of "phase scintillation" for the needs of our comparison.

The propagation from Σ_1 to Σ_2 (fig. 1) is described by a convolution with the free space impulse response $h_{z(x)}$ (GASKILL, 1978) in the Fresnel approximation:

$$B''(x) = B'(x) \otimes h_{z(x)} = \{(1 + i\phi_{(x)})\, B_{(x)}\} \otimes h_{z(x)} \qquad (10)$$

$$h_{z(x)} = (i\lambda z)^{-1} \exp\,(ik_0 x^2/2z).$$

The resulting intensity distribution in Σ_2 is to first order in ϕ

$$I_{(x)} = \left|B_{(x)} \otimes h_{z(x)}\right|^2 + \Delta I_{(x)}$$

where

$$\Delta I_{(x)} = -i\left(B_{(x)} \otimes h_{z(x)}\right)\left(\phi_{(x)}B^{*}_{(x)} \otimes h^{*}_{z(x)}\right) + c.c.$$

c.c is the complex conjugate of the immediately preceeding term. The near field being defined by $B_{(x)} \otimes h_{z(x)} \simeq B_{(x)}$,

$$\Delta I_{(x)} \simeq -iB_{(x)}\left(\phi_{(x)}B^{*}_{(x)} \otimes h^{*}_{z(x)}\right) + c.c. \quad . \tag{11}$$

The intrumental impulse response $h_{i(x,y)}$ is obtained by setting $\phi(x) = \delta_{(x-y)}$ in eq. (11):

$$h_{i(x,y)} \simeq -2(\lambda z)^{-1}\, B_{(x)}B^{*}_{(y)} \cos\{k_0(x-y)^2/2z\} \quad . \tag{12}$$

Over an area where $B_{(x)} \simeq B_{(y)}$ and $|B_{(x)}| \simeq \sqrt{I_0}$, the system is shift invariant with impulse response and transfer function (fig. 4.c & c'):

$$h_{i(x-y)} = h_{i(u)} \simeq -2(\lambda z)^{-1}\, I_0 \cos\{k_0u^2/2z\} \tag{13}$$

$$H_{(k)} = \widetilde{\Delta I}_{(k)}/\widetilde{\phi}_{(k)} \simeq 2I_0 \sin\{zk^2/2k_0\} \tag{14}$$

The discussion of the sensitivity of this technique at long wavelength (e.g. of the order of the beamwidth) is delicate, because, in order to obtain high sensitivity one would have to choose z too large to satisfy the near field condition $B_{(x)} \otimes h_{z}(x) \simeq B_{(x)}$. It could then not even loosely be associated with imaging.

3.3) The wavefront shearing interferometer

Another possibility of deriving a reference from the probe team is to set up an interferometric arrangement in which the phase at each point is measured with respect to a reference point within the beam. The position of that reference can be fixed or depend on the point where the measurement is made, as it is the case of the Bates wavefront shearing interferometer (BORN and WOLF, 1959). After its passage through the phase object the probe beam enters a Mach-Zehnder arrangement, at the output of which the beams from the two arms are superposed with a shear. Suitably offset for fractional fringe observation the instrument measures the phase difference between points separated by the shear distance, a, yielding (fig. 4d & d')

$$h_{i(u)} = 1/2\ I_0(\delta_{(u-a/2)} - \delta_{(u+a/2)}) \qquad (15)$$

$$H_{(k)} = I_0\ \sin(ak/2). \qquad (16)$$

For $k < \pi/2a$ the difference can be identified with a derivative. The small wavenumber sensitivity is limited by the fact that the shear, a, cannot be made larger than the beam width.

4) Comparison of transfer properties

In fig. 4 the transfer properties of the three methods described can be compared to those of an ideal Mach-Zehnder interferometer. It was assumed that the techniques all make use of the same laser source and have the same probe beam width and magnification.

The interferometer (a,a') set to fractional fringe observation gives a direct measurement of $\phi_{(x)}$ independently of the wavenumbers. Consequently

$h_{i(u)} = 1/2\ I_0\delta_{(u)}$ and $H_{(k)} = 1/2\ I_0$, the factor 1/2 arising from the use of two beamsplitters. A common feature of all techniques that lack a reference beam external to the plasma is their insensitivity to absolute path length variations, i.e. $H_{(0)} = 0$ strictly. The finite beam width is responsible for a "dip" in $H_{(k)}$ around k=0, that is at least equal to the width of $B_{(k)}$. (This is also true for the sensitivity of far-field techniques without an external reference - see appendix).

The drop in sensitivity for wavelength longer than the beam width is however not a handicap with respect to the interferometer, if we are only interested in fluctuations with wavelengths shorter than the beamwidth. On the contrary, such an instrument has the advantage of being considerably less sensitive to mechanical perturbations. Depending on the experimental situation, the removal of the large contribution to $\phi_{(x,t)}$ due to the bulk density of the plasma, may also be welcome.

Whereas for $k > k_c$ a phase contrast device can be treated like an interferometer, the interpretation of data obtained from a phase scintillation setup is much less straightforward. Its transfer function can take any value between $-2I_0$ and $+2I_0$. The zeros of $H_{(k)}$ represent lost information. Nonetheless, for $k^2 < |2k_0 z^{-1}|$ the approximation $H_{(k)} \simeq I_0 z k_0^{-1} k^2$ holds, showing that at long wavelength (or small z) it yields a measurement of $\partial_x^2 \phi_{(x)}$, exactly as the classical technique of shadowgraphy (JAHODA, 1971). The advantage of the technique seems to be in its simplicity, and, as it requires only few optical components, its high mechanical stability.

The wavefront shearing interferometer is easier to interpret and more sensitive at small k, due to the linear dependence of $H_{(k)}$ around k=0. Evidently, the phase contrast method provides both the highest overall

sensitivity and the closest approximation to the transfer function of an interferometer. In the appendix we show that a phase contrast device can provide a good physical realization of what could be regarded as an ideal "internal reference interferometer". Using a 23 cm wide probe beam, the system on the TCA tokamak has been shown to provide a flat response to wavelengths up to about 20 cm (WEISEN, 1985). The cutoff wavenumber k_c is adjustable, allowing one to reject unwanted spectral contributions. A disadvantage of the technique is that it needs high quality optics, otherwise its low-k performance is degraded by the broadening of the focal spot at the phase plate.

5) A direct experimental comparison between phase contrast and phase scintillation

The experiment reported here was carried out during the development of the phase contrast system now operating on the tokamak TCA (WEISEN, 1985-2). The gaussian beam of an 8 Watt CO_2 laser (λ = 10.6 μ) was suitably expanded to fill the 7x4 cm clear aperture of the optics with a FWHM of 4.8 cm (fig. 5). The parabolic mirror L_1 (f_1=45 cm) focussed the beam onto a phase mirror P, manufactured as described by WEISEN (1985). Mirror L_2 (f_2=27.5 cm) produced the final conjugation of the planes Σ and Σ'. Ultrasonic waves were produced by a piezoelectric transducer (with resonant frequencies between ~100 and 500 kHz) which could be scanned in the z direction along the beam. When the groove (width 200 μ) of the phase mirror was positioned to coincide with the focal spot, the system operated in the "phase contrast mode". When it was shifted out of coincidence, the groove was of no effect and the system operated in the "scintillation mode".

The homodyne interference signals due to the ultrasonic waves were

detected by a liquid nitrogen cooled HgCdTe photovoltaic diode at Σ'. A fast lock-in amplifier yielded their vector amplitude and relative phase as a function of the transducer position. Fig. 6 shows the amplitude obtained for 3 successive scans with k= 37.3 rad/cm in each of the two modes of operation. As expected, when the transducer was at Σ (i.e. z=0), there was no signal in the scintillation mode, whereas phase contrast was at its maximum. The peak sensitivities were the same in both cases. Zero crossings were always accompanied by inversals of the signals. The distance $d_{(k)}$ between successive zero crossings (fig. 7) was as predicted by eq. (14), i.e.

$$d_{(k)} = 2\pi k_0 k^{-2} = \Lambda^2 \lambda^{-1}$$

The same results were obtained for a phase scintillation arrangement without imaging optics (as in fig. 1a), the detector being placed at the position of L_1. (The advantage of imaging optics for a practical scintillation device are that they allow one to choose the magnification of the system and to set the effective detection plane Σ_2 (fig. 1.a) at otherwise inaccessible positions.)

6) Depth of field

As seen from fig. 6 phase contrast is subject to scintillation effects when the imaging is out of focus. This effect is easily taken into account if an additional modulation factor $\cos\{zk^2/2k_0\}$ is introduced into the right hand side of eq. (9). Under these conditions an interferometer will also suffer scintillation effects, as reported by SHARP (1983). As these effects are basically undesirable for the operation of imaging diagnostics, the length 1/2 $d_{(k)}$ will be a measure of the allowable depth of field, defined between the points where the sensitivity drops to 70% of its in focus value.

The resulting requirement

$$|z| \leq \Lambda^2/4\lambda \qquad (17)$$

is similar to the requirement that the Klein & Cook parameter Q be small to ensure Raman-Nath diffraction (KLEIN and COOK, 1967). For a plasma with a diameter of 40 cm, (17) is satisfied for $\Lambda \geq 0.3$ cm if a CO_2 laser (λ = 10.6 μ) is used. It is however only satisfied when $\Lambda \geq 3$ cm for a probe beam in the FIR with λ = 1 mm. Thus for imaging techniques, the use of a short probe wavelength results in the advantage of a wider range of plasma wavelengths that can be studied.

7) Summary

Imaging methods are in general better suited to the study of long wavelength fluctuations than scattering techniques. In order to obtain information about large scale fluctuations it is necessary to have a wide access to the plasma. If possible the probe beam should be as wide as the plasma. For wavelengths smaller than the beam width, imaging methods using no external reference beam can provide information that is equivalent to that given by an interferometer, with the advantage of simplicity and reduced sensitivity to mechanical perturbations. This advantage is particularly welcome if one uses a CO_2 laser to obtain a large depth of field. The transfer function of the phase contrast method is the closest approximation to the wavenumber independent transfer function of the interferometer. For wavelength larger than the beam width, the sensitivity of methods that do not use an external reference beam decreases in the same way than for far field methods.

Other imaging methods may still need to be discovered or rediscovered to suit particular applications.

Acknowledgements

The author thanks Dr. R. Behn, Dr. P.D. Morgan, Prof. F. Troyon, Prof. R. Stern, Dr. M. Siegrist, Dr. J.B. Lister, Dr. J. Vaclavik, Dr. F. Jahoda and the members of the TCA team for many stimulating discussions.

References

BORN M. and WOLF E., Principles of Optics, Pergammon Press, (1959)

EVANS D.E., Von HELLERMANN M., HOLZHAUER E., Plasma Physics 24, 819 (1982)

GASKILL G., Linear Systems, Fourier transforms and Optics Wiley, New York (1978)

HUGENHOLTZ C.A.J. and MEDDENS B.J.H., Rev. Scient. Instrum. 53, 171 (1982)

JAHODA F.C., in Methods of Experimental Physics, Vol. 9, part B, ed. Lovberg and Griem, Academic Press (1971)

JAMES B.W. and YU C.X., Plasma Phys. and Contr. Fusion 27, 557 (1985)

KLEIN W.R. and COOK B.D., IEEE Transactions on Sonics and Ultrasonics, SU-14, No 3, 123 (1967)

PRESBY H.M. and FINKELSTEIN D., Rev. Sci. Instrum. 38, 1563 (1967)

SHARP L.E., Plasma Physics 25, 781 (1983)

SLUSHER R.E. and SURKO C.M., Physics of Fluids 23, 472 (1980)

SONODA Y., SUETSUGU Y., MURAOKA K., AKAZAKI M., Plasma Physics 25, 1113 (1983)

TFR GROUP and TRUC A., Plasma Phys. and Contr. Fusion 26, 1062 (1984)

WEISEN H., CRPP report INT 108/82, Lausanne (1982)

WEISEN H., Infrared Physics 25, 543 (1985)

WEISEN H., Proceedings of the 2nd International Symposium on Laser-Aided Plasma Diagnostics, Culham 10-12 Sept. (1985)

YOUNG P.E., NEIKIRK D.P., TONG P.P., RUTLEDGE D.B., and LUHMANN N.C., Rev. Sci. Instrum. 56, 81 (1985)

ZERNIKE F., Z. Tech. Phys. 16, 454 (1935)

Figure captions

Fig. 1 a) diffraction by a thin phase object
b) complex amplitude diagram of the transmitted wave
c) detection of a small phase shift by adding an external reference wave (interferometry)
d) homodyne detection of a small phase shift with an internal reference.

Fig. 2 Basic setup for phase-contrast
Σ, object plane
Σ', image plane
P, phase plate
D, diffracted light component
UD, undiffracted light component
L_1 and L_2, focussing and imaging lenses

Fig. 3 Wavenumber response of the phase contrast method from eq. (5).

Fig. 4 Compared impulse and wavenumber responses for the 4 methods discussed
a,a') interferometry
b,b') phase contrast
c,c') phase scintillation
d,d') wavefront shearing interferometry

Fig. 5 Experimental setup used to compare phase contrast and phase scintillation. Captions as for fig. 2, except
T, piezoelectric ultrasonic transducer
DT, HgCdTe detector element

Fig. 6 Amplitude of the interference term for phase contrast (1) and phase scintillation (2) as a function of the transducer position z.

Fig. 7 Distance $d_{(k)}$ between zero crossings.

Fig. 8 (1) Normalised wavenumber response $H_{(k)}/2I_0$ from eq. (A.7)
(2) Maximum homodyning efficiency η_{max} from eq. (A.12).

APPENDIX

Long wavelength limitations

We first present a theoretically ideal "internal reference interferometer" and then show that the drop of the sensitivity at small $|k|$ is a general feature of any method (imaging, near-field, far-field) using no reference beam exterior to the plasma.

We start from eq. (1)

$$\begin{aligned} B'_{(x)} &= B_{(x)} + iD_{(x)} \\ &= B_{(x)} + i\phi_{(x)}\, B_{(x)} \end{aligned} \tag{A.1}$$

where $B_{(x)}$ and $\phi_{(x)}$ are arbitrary (but $|\phi_{(x)}| \ll 1$) and belong to the space of square-integrable complex functions. The interaction of the incident beam with a phase object must conserve the total power

$$\|B\|^2 \equiv \int B^*_{(x)} B_{(x)} dx = \|B'\|^2, \tag{A.2}$$

implying

$$\int (iD_{(x)} B^*_{(x)} + c.c.)dx = 0. \tag{A.3}$$

We now decompose $D_{(x)}$ into its components in the subspace $E_\parallel$ generated by $B_{(x)}$ and the perpendicular subspace $E_\perp$.

$$D_\parallel(x) = \frac{\int B^*_{(v)} D_{(v)} dv}{\int B^*_{(v)} B_{(v)} dv}\; B_{(x)} \equiv \alpha B_{(x)}$$

$$D_\perp(x) = D_{(x)} - D_\parallel(x)$$

It follows from eq. (A.3) that α is imaginary. Hence, whatever linear operation is performed on $B'_{(x)}$, the interference between diffracted and undiffracted light will contain no contribution due to $D_{\parallel(x)}$. An ideal "internal reference interferometer" can still be thought to make use of all of the available diffracted light (i.e. the $D_{\perp}$ components) and produce intensity variations $\Delta I_{(x)}$ consistent with (A.3) given by

$$\Delta I_{(x)} = B^{*}_{(x)} D_{\perp(x)} + c.c.$$

$$= 2B^{*}_{(x)} B_{(x)} \left\{ \phi_{(x)} - \frac{\int B^{*}_{(v)} B_{(v)} \phi_{(v)} dv}{\int B^{*}_{(v)} B_{(v)} dv} \right\} \qquad (A.5)$$

for $\phi_{(x)}$ real.

As can be seen from this equation, $\Delta I_{(x)}$ is a measure of the phase $\phi_{(x)}$ with respect to a weighted average of $\phi_{(x)}$. In this ideal case the weighting function is the normalized intensity profile of the beam. Phase differences between any two points are measured as well as with a classical interferometer. It is easily verified that the intensity variations of eq. (A.5) are produced by a linear imaging system modeled by a unitary operator $\underline{U}$ having the eigenvalue 1 in the subspace $E_{\parallel}$ and all eigenvalues equal to $-i$ in $E_{\perp}$.

$$\underline{U} : B'_{(x)} \rightarrow B''_{(x)} = B_{(x)} + iD_{\parallel(x)} + D_{\perp(x)} \qquad (A.6)$$

In the shift invariant approximation around x=0, (A.5) leads to a transfer function similar to eq. (9):

$$H_{(k)} = 2I_0 \left\{ 1 - \frac{\int \tilde{B}_{(l)} \tilde{B}^{*}_{(l-k)} dl}{\int \tilde{B}_{(l)} \tilde{B}^{*}_{(l)} dl} \right\}$$

$$= 2I_0 \{1 - \frac{\tilde{B}_{(k)} \otimes \tilde{B}^*_{(-k)}}{\tilde{B}_{(1)} \otimes \tilde{B}^*_{(-1)}}\Big|_{1=0}\} \qquad (A.7)$$

We see that a phase contrast device using a phase mirror with k_c closely matched to the diffraction limited spot size is a good approximation to the ideal instrument described by eqs. (A.5) and (A.7). Fig. (8) shows $H_{(k)}/2I_0$ in the case where $B_{(x)} = \exp(-x^2/2w^2)$. (Note that the absence of a first order dependence of $H_{(k)}$ is particular to x=0.)

The transfer function of a shift invariant imaging device can also serve for a comparison with the wavenumber response defined for far-field techniques. Clearly there is no a priori difference in sensitivity between the two classes. However, for a system that is not shift invariant, the local wavenumber response (as defined in section 3) does not adequately describe the system's overall efficiency.

In the following we therefore give a more general upper limit to the total homodyne power, that can be obtained by methods relying on the undiffracted wave as a local oscillator.

The available diffracted power is $\|D_\perp\|^2 = \int D^*_\perp(v) D_\perp(v) dv$ and the total local oscillator power is $\|B\|^2 = \int B^*_{(v)} B_{(v)} dv$, yielding an interference signal of power

$$\Delta P \leq 2\|D_\perp\| \|B\| \leq 2\|D\| \|B\| \qquad (A.8)$$

The highest homodyning efficiency of an "internal reference apparatus" is thus

$$\eta_{max} = \frac{\|D_\perp\|}{\|D\|} = \sqrt{1 - \frac{\|D_\parallel\|^2}{\|D\|^2}} \qquad (A.9)$$

$$\text{or} \quad \eta_{max} = \{1 - \frac{\left|\int B^*_{(v)} B_{(v)} \phi_{(v)} dv\right|^2}{[\int B^*_{(v)} B_{(v)} dv][\int \phi^*_{(v)} \phi_{(v)} B^*_{(v)} B_{(v)} dv]}\}^{1/2} \qquad (A.10)$$

For a perturbation of the form $\phi_{(x)} = \exp(ikx)$ this reduces to

$$\eta_{max(k)} = \{1 - \frac{\left|\tilde{B}_{(k)} \otimes \tilde{B}^*_{(-k)}\right|^2}{\left|\tilde{B}_{(l)} \otimes \tilde{B}^*_{(-l)}\right|^2_{l=0}}\}^{1/2} \qquad (A.11)$$

If $B_{(x)}$ is a gaussian beam of the form $B_{(x)} = \exp(-x^2/2w^2)$, then (fig. 8)

$$\eta_{max(k)} = \{1 - \exp(-k^2w^2/2)\}^{1/2} \qquad (A.12)$$

There is a "dip" of sensitivity at small wavenumbers, the width of which is at least equal to the width of $\tilde{B}_{(k)}$. As $\phi_{(x)}$ and $B_{(x)}$ were taken to be complex (rather than real) functions, the result can be extended to the case of diffraction that does not occur in the Raman-Nath regime and to the common detection schemes where the probe and the local oscillator beams cross inside the scattering volume.

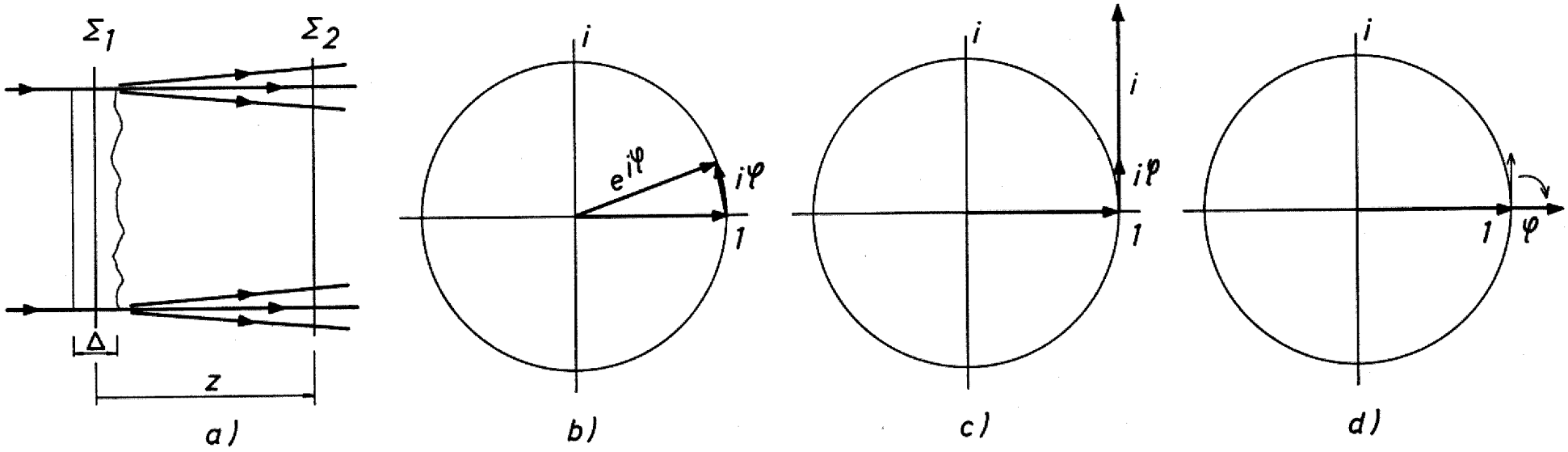
Σ_1
Σ_2
Δ
z
a)
i
$e^{i\varphi}$
$i\varphi$
1
b)
i
i
$i\varphi$
1
c)
i
1
φ
d)

fig. 1

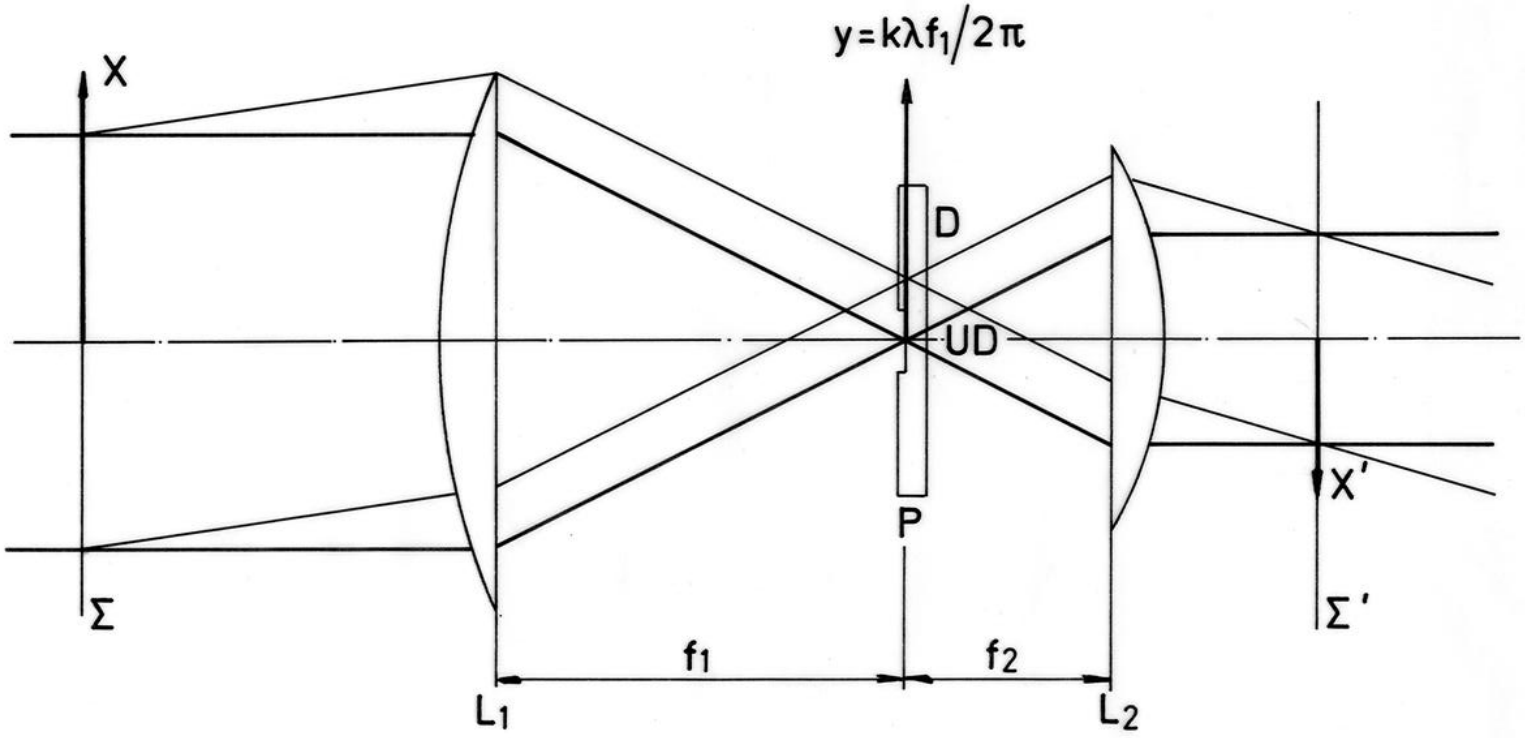

fig. 2

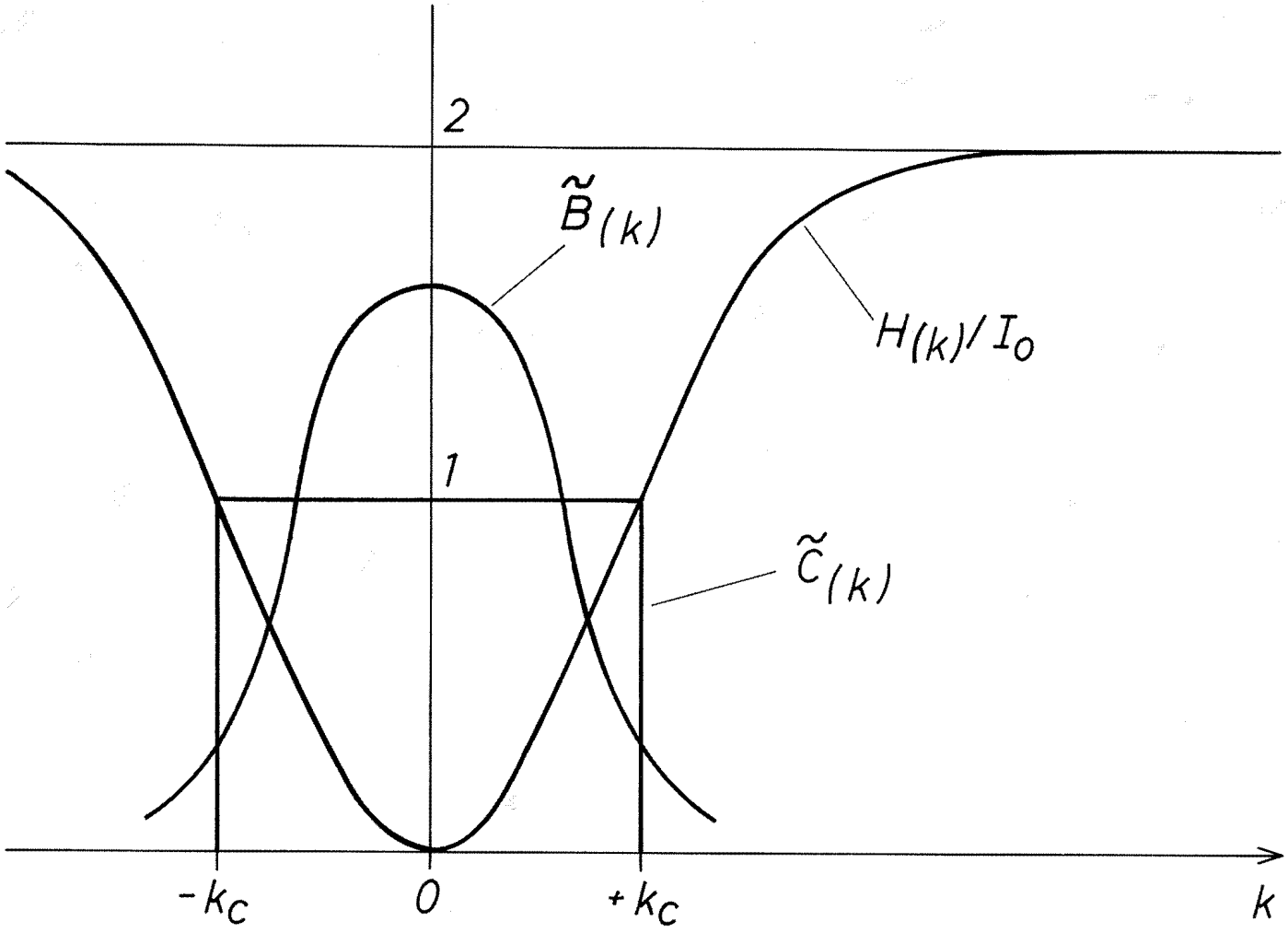

fig. 3

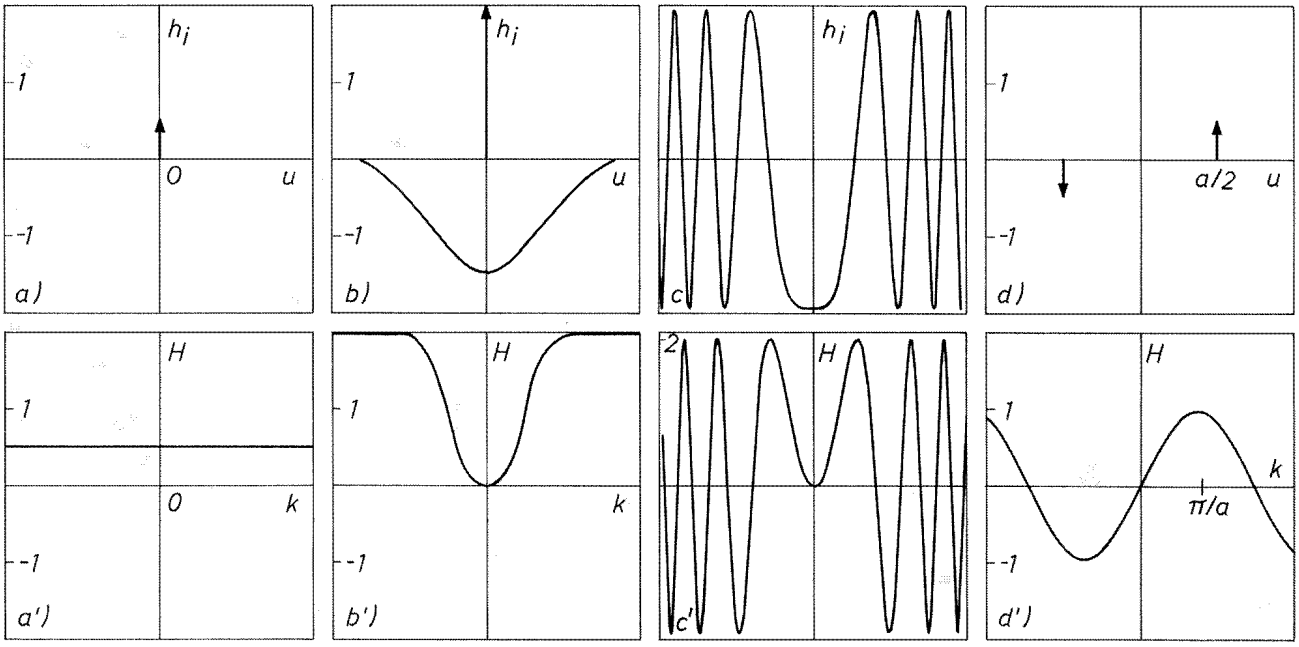

fig. 4

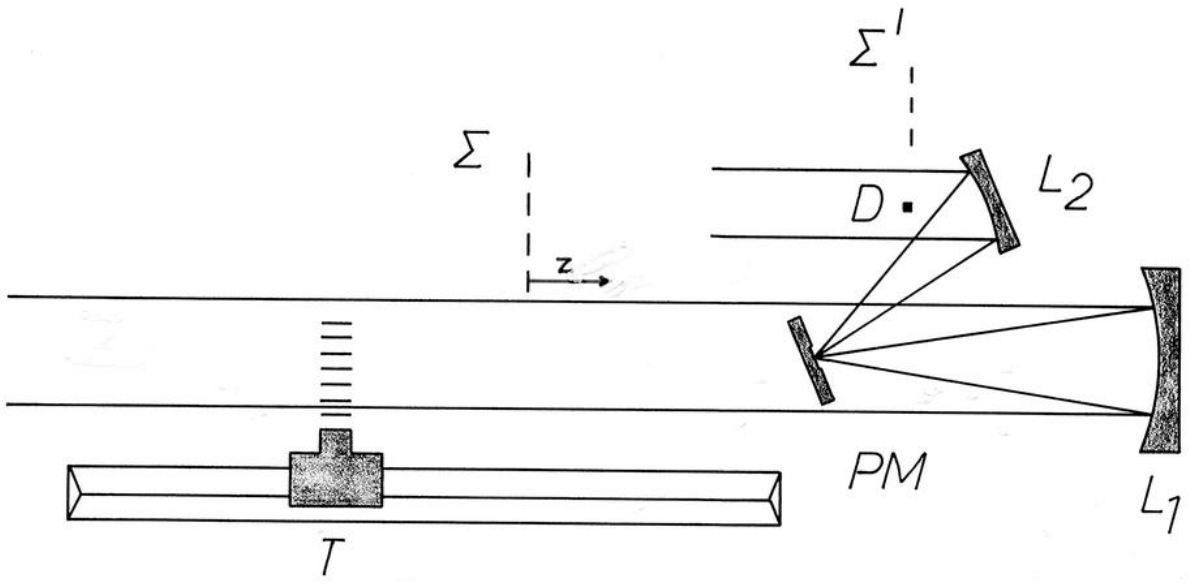

fig. 5

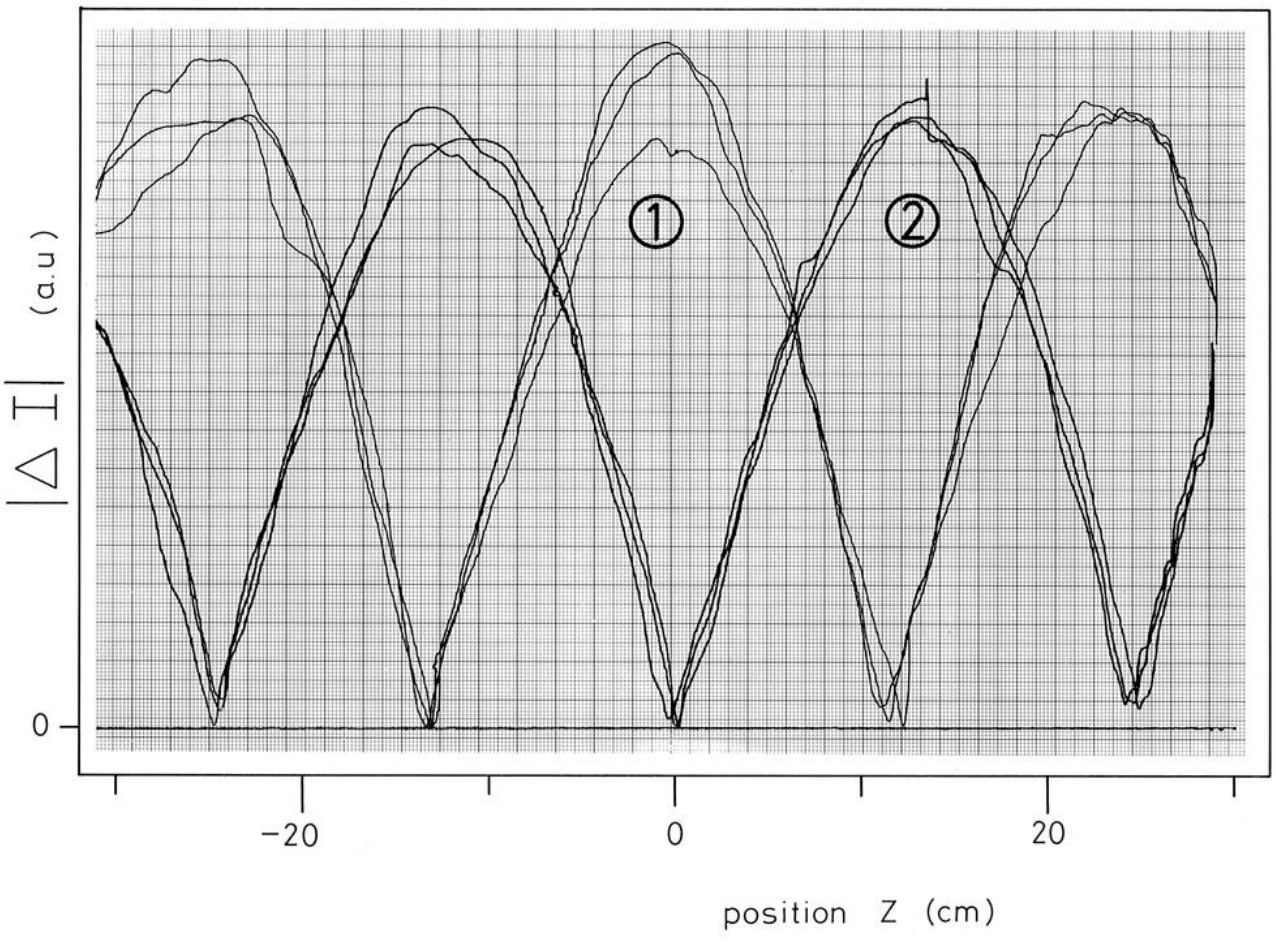

fig. 6

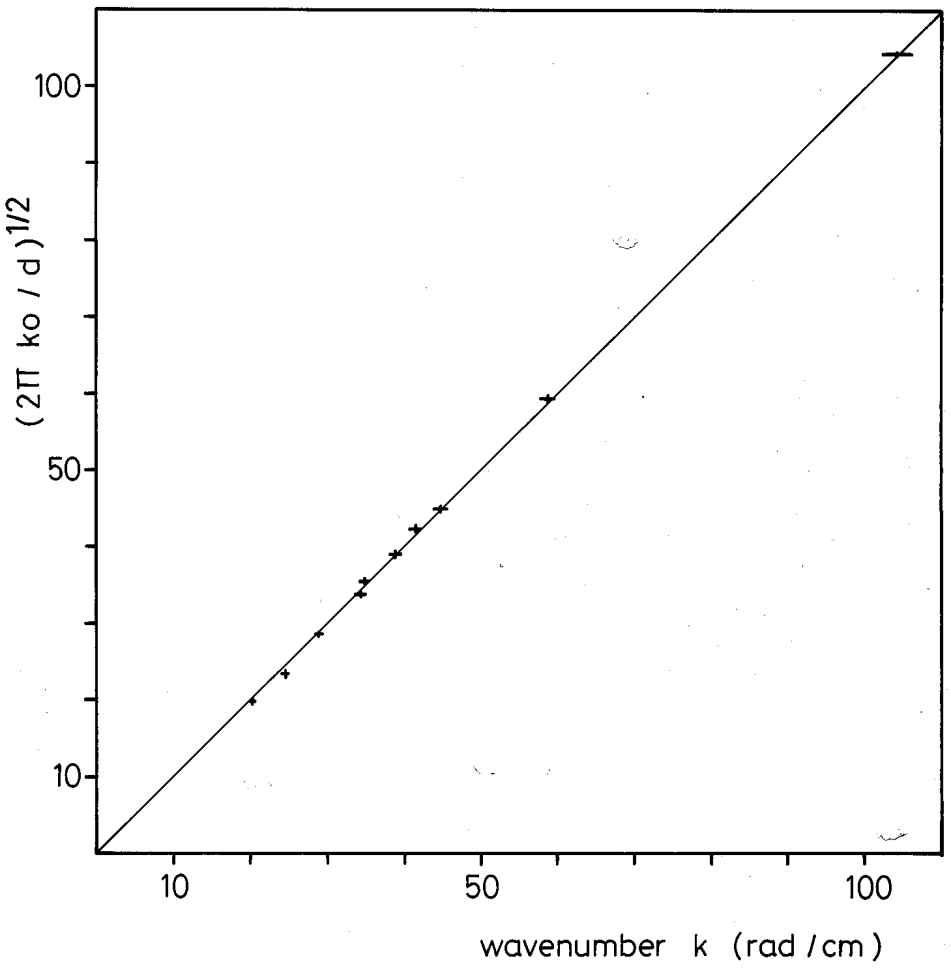

fig. 7

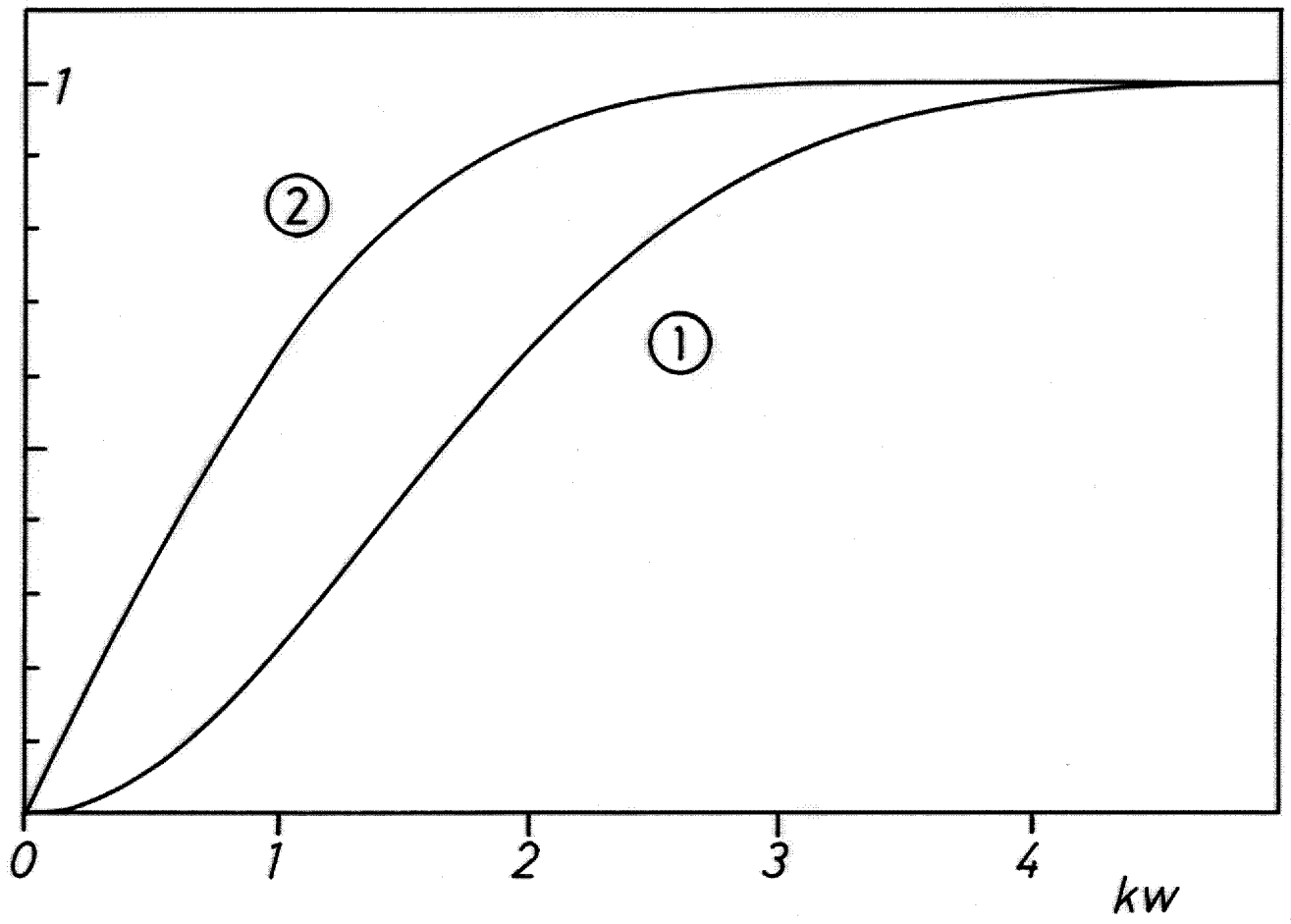

fig. 8